

Purdue University

Purdue e-Pubs

International Compressor Engineering
Conference

School of Mechanical Engineering

1994

A Method for Computing the Compression Loads in Twin Screw Compressors

G. P. Adams
University of Arkansas

W. Soedel
Purdue University

Follow this and additional works at: <https://docs.lib.purdue.edu/icec>

Adams, G. P. and Soedel, W., "A Method for Computing the Compression Loads in Twin Screw Compressors" (1994). *International Compressor Engineering Conference*. Paper 958.
<https://docs.lib.purdue.edu/icec/958>

This document has been made available through Purdue e-Pubs, a service of the Purdue University Libraries.
Please contact epubs@purdue.edu for additional information.
Complete proceedings may be acquired in print and on CD-ROM directly from the Ray W. Herrick Laboratories at
<https://engineering.purdue.edu/Herrick/Events/orderlit.html>

A METHOD FOR COMPUTING THE COMPRESSION LOADS IN TWIN SCREW COMPRESSORS

G.P. Adams
University of Arkansas
Mechanical Engineering Department
Fayetteville, AR 72701

Werner Soedel
Purdue University
1077 Herrick Laboratories
West Lafayette, IN 47907

ABSTRACT

An important consideration in the design and analysis of a twin screw compressor is the computation of the rotor loads due to the compression process. A method for computing these compression loads is presented here. The compression process is viewed as a quasi-static, polytropic process. The forces and moments on each rotor are computed as a function of the angular position of the rotor. The compression loads are computed by integrating the pressure over the rotor surface. The 3-D helical rotor surface is mapped to a 2-D region for computing the integrals. The boundaries of the integration region are defined by the various seal geometries. These include the rotor faces at the suction and discharge planes, the compressor housing/lobe tip seal, and the interlobe seal curve. The Cartesian coordinate system used here results in forces in the principal directions and moments taken about the center of the rotor, in the suction plane. These forces and moments are then resolved to the bearing locations. Compression loads for a typical operating condition are presented. In general it is noted that the magnitude of the moment about the axis of rotation on the female rotor is approximately 12% of that on the male rotor. This algorithm provides for the inclusion of the compression loads in a model used to simulate the rotor motion.

INTRODUCTION

This work is based on research conducted by the authors while at Purdue University [1]. As used throughout this paper, the term *compression loads* refers to the forces and moments induced on the rotors of a screw compressor due to the compression of the gas only. Dynamic effects are not included here. Rather the loads are computed as a function of the angular position of the rotor. The compression loads can then be used to model the rotor dynamics during the compression process [2]. Therefore, the bearing loads which exist within the mechanism can be computed.

An overview of the computation method is first presented, followed by a review of the vector calculus which is used. Some details of the implementation are provided for the geometry associated with twin screw compressors. The authors [3] have previously published related work in which the interlobe seal curve is approximated as a straight line parallel to the rotor axis of rotation. In this work, the actual interlobe seal geometry is used, avoiding the inaccuracy associated with the straight line approximation.

THE INTEGRATION METHOD

Three geometric constructions, *sections*, *chambers* and *strips*, are used in computing the compression loads for the screw compressor rotors. The male rotor is divided into N_m equivalent *sections*, where N_m is the number of lobes on the male rotor. These sections are bounded by adjacent lobe tips, and extend from the suction plane to the discharge plane. Figure 1 is a view of the male rotor with a single section emphasized. The contact points between the male and female rotors form an interlobe seal curve along the male rotor. This interlobe seal curve, shown for one section in Figure 1, further divides the N_m sections of the male rotor into separate compression *chambers*. A low pressure chamber extends from the suction plane to the seal curve along the top of the rotor. A high pressure chamber extends from the seal curve to the discharge plane along the bottom of the

rotor. The compression loads are computed by integrating the pressure over the surface defined by each chamber. The required integrations are performed by further dividing each chamber into helical *strips* and summing the integrals computed over each strip.

The compression in each chamber is assumed to be a polytropic process in which the pressure is constant throughout each individual chamber for a specific rotor position. The chamber pressure is therefore a scalar which can be integrated over the surface of the rotor by mapping each 3-D compression chamber into a 2-D integrating region. The integrands and associated limits used to compute the compression loads are functions only of the chamber geometry, as defined by the rotor surface and the various seal interfaces. Due to the symmetry of the rotors, the compression loads are defined for all values of θ_m , by computing the loads for values of θ_m from 0.0 to $2\pi/N_m$.

Integration of a Scalar Over a Surface

The general integration procedure is described here. Let a surface, S , be defined in terms of two variables, u and v . The integral of a scalar over the surface can be defined over a 2-D region as

$$\int_S \int f \, ds = \int_R \int f \, ||\vec{T}_u \times \vec{T}_v|| \, du \, dv \quad (1)$$

where

$$S = \text{the surface definition; } S_x \vec{i} + S_y \vec{j} + S_z \vec{k} \quad (2)$$

$$ds = \text{elemental surface area} \quad (3)$$

$$R = \text{the integrating region} \quad (4)$$

$$f = \text{scalar value} \quad (5)$$

$$u \text{ and } v = \text{2-D mapping parameters} \quad (6)$$

$$\vec{T}_u \text{ and } \vec{T}_v = \text{surface tangent vectors.} \quad (7)$$

In order to implement this method to compute the compression loads, the scalar quantity, f , becomes the pressure, P , in a given chamber, multiplied by the appropriate component of the surface normal vector, $\vec{n} = \frac{(\vec{T}_u \times \vec{T}_v)}{||\vec{T}_u \times \vec{T}_v||}$. The x -component forces and moments due to compression are computed as

$$F_x = P \int \int n_x ||\vec{T}_u \times \vec{T}_v|| \, du \, dv = P \int \int (\vec{T}_u \times \vec{T}_v)_x \, du \, dv \quad (8)$$

$$M_x = P \int \int (\vec{T}_u \times \vec{T}_v)_z S_y - (\vec{T}_u \times \vec{T}_v)_y S_z \, du \, dv. \quad (9)$$

Similar equations apply for the y and z components.

INTEGRATION METHOD APPLIED TO THE ROTORS

The integration method described above is applied to the screw compressor rotors by defining a suitable mapping. Assumptions are made about the nature of the discrete polar coordinates which define the rotor profiles.

Mapping the 3-D Rotor Surface to a 2-D Region

The Cartesian coordinate system used for mapping the 3-D surface to a 2-D region and the required variable definitions are shown in Figure 2. The origin of the Cartesian coordinate system is the point defined by the rotational axis of the male rotor, the center of the 2-D profile, at the suction plane.

The 3-D rotor geometry is completely defined by the 2-D profile, the length of the rotor, L , and the wrap angle, τ_m , of the rotor. The 2-D profile is defined by the discrete polar coordinates, β_m and Θ_m , of one lobe. The symmetric profile is completed by incrementing these polar coordinates appropriately to define N_m lobes. Using these geometric parameters, the 2-D integration variables can be defined. The parameters θ and ϕ are used as the integrating variables.

The variable θ is the unique polar coordinate associated with each point on the 2-D rotor profile. For the i^{th} point, this coordinate is defined in terms of the profile data coordinate $\Theta_m(i)$, the specific section involved $sect$, and the current rotational position, θ_m , of the rotor.

$$\theta = \Theta_m(i) + \theta_m + (sect - 1) \left(\frac{2\pi}{N_m} \right) \quad (10)$$

The 2-D profile is not known in closed form but only as a set of discrete polar coordinates. The radius of the rotor is defined in terms of the discrete polar coordinates by assuming that the radius varies linearly as a function of Θ_m between adjacent points. This can be used to define $R(\theta)$ for the entire 2-D profile.

$$R_m(\delta) = R_m(i) + \beta_m(i) (\delta - \Theta_m(i)) \quad (11)$$

where

$$\begin{aligned} \Theta_m(i) &\leq \delta \leq \Theta_m(i+1) \\ \beta_m(i) &= \frac{R_m(i+1) - R_m(i)}{\Theta_m(i+1) - \Theta_m(i)} \end{aligned}$$

The variable ϕ is related to the amount of twist associated with a specific integration region. Its limits are defined by the seals which bound the region. Therefore, the value of ϕ varies from 0.0 to $-\tau_m$.

Resulting Integrals

The integration variables, θ and ϕ , completely define the 3-D rotor surface. The Cartesian coordinates of the rotor surface are defined in terms of θ and ϕ as

$$S_x = R_m(\theta) \cos(\theta + \phi) \quad (12)$$

$$S_y = R_m(\theta) \sin(\theta + \phi) \quad (13)$$

$$S_z = (L/\tau_m) \times \phi. \quad (14)$$

In addition, the cross product of the tangent vectors, $(\vec{T}_u \times \vec{T}_v)$, becomes

$$\vec{T}_\phi \times \vec{T}_\theta = (-L/\tau_m) \{ \beta_m \sin(\theta + \phi) + R_m(\theta) \cos(\theta + \phi) \} \vec{i} \quad (15)$$

$$+ (L/\tau_m) \{ \beta_m \cos(\theta + \phi) - R_m(\theta) \sin(\theta + \phi) \} \vec{j} \quad (16)$$

$$+ \beta_m R_m(\theta) \vec{k}. \quad (17)$$

Using this mapping scheme, the compression loads can be computed. The resulting integrations are

$$F_{x_m} = -P(L/\tau_m) \int \int \{ \beta \sin(\theta + \phi) + R_m(\theta) \cos(\theta + \phi) \} d\phi d\theta \quad (18)$$

$$F_{\theta_m} = P(L/\tau_m) \int \int \{ \beta \cos(\theta + \phi) - R_m(\theta) \sin(\theta + \phi) \} d\phi d\theta \quad (19)$$

$$F_{z_m} = -P \int \int \beta R_m(\theta) d\phi d\theta \quad (20)$$

$$M_{x_m} = -P \int \int \beta R_m(\theta) \{ R_m(\theta) \sin(\theta + \phi) \} d\phi d\theta \\ -P(L/\tau_m)^2 \int \int \{ \beta_m \cos(\theta + \phi) - R_m(\theta) \sin(\theta + \phi) \} \phi d\phi d\theta \quad (21)$$

$$M_{y_m} = P \int \int \beta R_m(\theta) \{ R_m(\theta) \cos(\theta + \phi) \} d\phi d\theta \\ -P(L/\tau_m)^2 \int \int \{ \beta_m \sin(\theta + \phi) + R_m(\theta) \cos(\theta + \phi) \} \phi d\phi d\theta \quad (22)$$

$$M_{z_m} = P(L/\tau_m) \int \int \beta R_m(\theta) d\phi d\theta \quad (23)$$

Integral Limits

The integration is performed by dividing each chamber into helical strips along the rotor surface. The boundaries which define these strips are

1. The arc subtended by adjacent discrete profile points at the suction plane,
2. Helical lines extending from the adjacent discrete profile points at the suction plane to the location of the corresponding points at the discharge plane,
3. The intersections of the helical lines with the interlobe seal curve,
4. The arc subtended by adjacent discrete profile points at the discharge plane.

The integrands and limits of integration required to compute the compression loads are dependent on the specific value of θ_m , the rotation of the male rotor. The integrations are performed at incremental values of θ_m , from 0.0 to $2\pi/Nm$, for the series of helical strips which define each individual chamber, within the N_m sections of the rotor. The summation of the integrations for each chamber results in the compression loads for the entire rotor at each incremental value of θ_m .

CONCLUSIONS

Typical bearing loads which result from the compression forces are presented in Figures 3 to 5. The moments about the rotor axes, M_{z_m} and M_{z_f} , exhibit an important characteristic of the compression loadings present in the screw compressor. The magnitude of M_{z_f} is approximately 12% of the magnitude of M_{z_m} . This effect is caused by the shape of the interlobe seal curve and the resulting projected area of each rotor which is exposed to the various chamber pressures. The effect is also evident in the axial forces, F_{z_m} and F_{z_f} . Due to the significant difference in the axial moment values, the female rotor tends to behave more like an idler, effectively un-loaded, than a member of a gear train.

ACKNOWLEDGMENTS

The authors would like to acknowledge United Technologies, Carrier Corporation for sponsoring the research program which made these efforts possible.

REFERENCES

- [1] G. P. Adams. *Modelling and Computer Simulation of Rotor Chatter and Oscillating Bearing Loads in Twin Screw Compressors*. PhD thesis, Purdue University, Purdue University W. Lafayette, IN 47907, December 1993.
- [2] G.P. Adams and Werner Soedel. Dynamic simulation of rotor contact forces in twin screw compressors. In Woerner Soedel, editor, *1994 International Compressor Engineering Conference at Purdue*, Herrick Laboratories, West Lafayette, IN, 47907, July 1994. Ray W. Herrick Laboratories, School of Mechanical Engineering, Purdue University.
- [3] G.P. Adams and Werner Soedel. Remarks on oscillating bearing loads in twin screw compressors. In James F. Hamilton, editor, *1992 International Compressor Engineering Conference at Purdue*, pages 439–447, Herrick Laboratories, West Lafayette, IN, 47907, July 1992. Ray W. Herrick Laboratories, School of Mechanical Engineering, Purdue University.

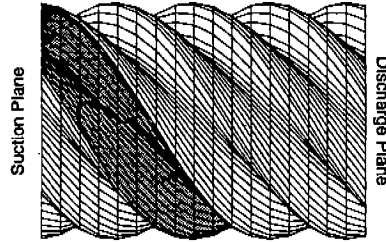


Figure 1: Interlobe Seal Curve on Male Rotor

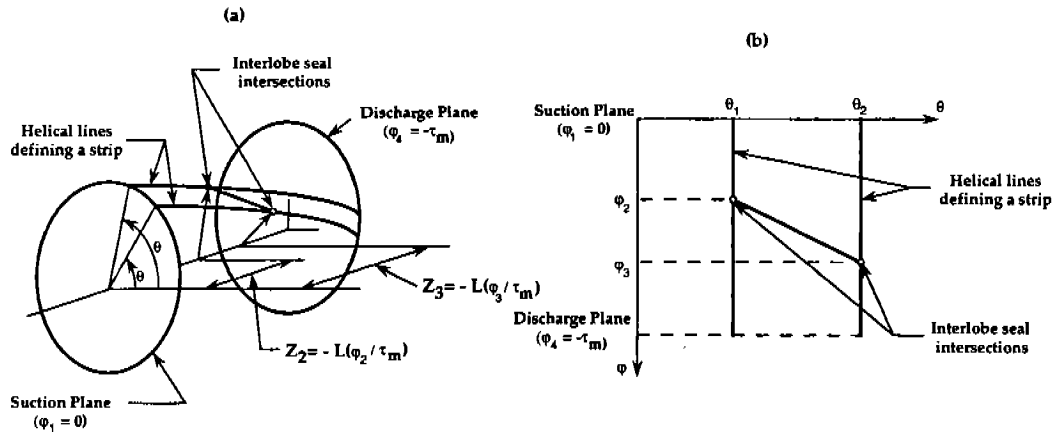


Figure 2: Mapping of 3-D rotor surface to a 2-D region. Demonstrated on a cylinder.

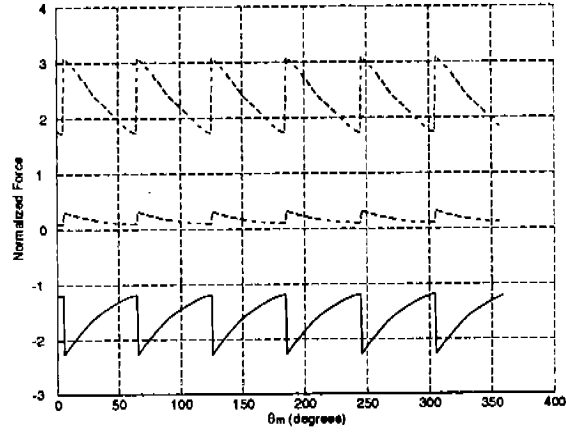


Figure 3: Suction bearing loads, male rotor, under pressure, $(-)$ X_m , $(---)$ Y_m , $(-\cdot-)$ Z_m .

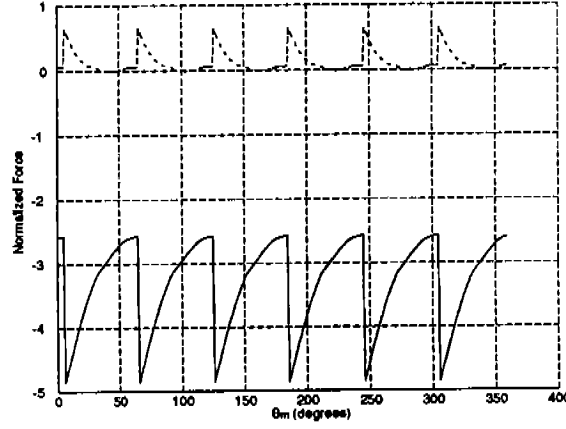


Figure 4: Discharge bearing loads, male rotor, under pressure, $(-)$ X_m , $(---)$ Y_m .

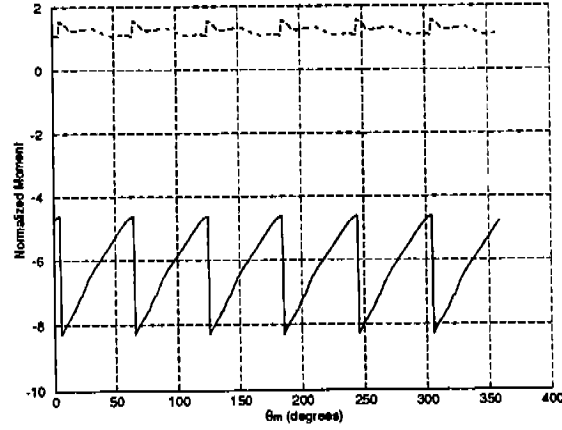


Figure 5: Moments about z-axis due to compression, under pressure, $(-)$ M_{zm} , $(---)$ M_{zf} .